

Separation and characterization of phases in bond percolation and implications for studies of nuclear multifragmentation

A. J. Cole

Institut des Sciences Nucléaires, IN2P3/CNRS, Université Joseph Fourier, 53 Av. des Martyrs, F-38026 Grenoble cedex, France

(Received 30 July 2001; published 5 February 2002)

We demonstrate that, in bond percolation of a small system, two phases can be visually identified by displaying the probability distribution of the ejected mass as a function of the number of broken bonds. The phases can be separated using the ratio of the masses of the second largest and largest fragments. The nature of the transition and application to studies of nuclear multifragmentation are discussed.

DOI: 10.1103/PhysRevC.65.031601

PACS number(s): 25.70.Pq, 25.70.Mn, 24.60.Ky

Several works have demonstrated the similarity between the bond or site percolation processes and nuclear fragmentation [1–3]. The bond percolation studies suggest that it is possible to define a temperature, T , in the nuclear system which corresponds approximately to the bond breaking probability, p , in percolation. At small p or T the “parent” system breaks into a few small particles together with a heavy residue (percolating cluster). In the nuclear case this process is well known and successfully described using statistical (evaporation) models [4,5]. As p or T increases, the size of the residue diminishes and, at a point which is often likened to a phase transition [6], can no longer be clearly identified. Beyond this point, the use of evaporation models (even those which allow for sequential emission of large fragments) is difficult to justify. The fragmented system is composed of light and intermediate size fragments which appear to be produced by an explosive multifragmentation mechanism [4,6–10].

We believe, with Gross [7], that small systems can be studied as specific problems in statistical mechanics rather than as scaled down analogs of “large” systems which may be conveniently approached using conventional thermodynamics. In this context we showed in [2] how to build a rather complete analogy between percolation and nuclear fragmentation by associating the excitation energy of the nuclear system with the number of broken bonds, N_b , in the percolation system. An important feature of this work was the equivalence of the effective thresholds ($-Q$ value +Coulomb barrier) in fragmentation with the Q values (expressed as a number of broken bonds) in percolation.

This analogy notwithstanding, it is impossible to establish an exact correspondence between the probability distribution of broken bonds expected for a system in contact with a heat reservoir and the binomial distribution obtained using a fixed bond breaking probability (this problem disappears for large systems). We further observe that such a reservoir cannot be identified in nuclear fragmentation except in the restricted sense that the contribution to the statistical weight of any given macrostate due to the (relatively few) degrees of freedom corresponding to fragment kinetic energies can be approximately estimated in this way [8,9].

It thus appears interesting to investigate the region of the percolation phase transition in small systems using a fixed number of broken bonds in each simulation run (for an introduction to percolation, see Stauffer and Aharony [11]). We

have, accordingly, performed simulations using a $5 \times 5 \times 5$ cubic system for which the total number of bonds (binding energy) is $N_T = 3 \times 5^2 \times (5 - 1) = 300$.

The fundamental quantities issuing from the simulations are the partition probabilities, $P\{\mathbf{n}\}$, where the vector, \mathbf{n} , symbolizes a partition of the total mass, M_T (which, in bond percolation is the total number of sites). Explicitly, $\mathbf{n} \equiv n_1, n_2, \dots, n_m, \dots, n_{M_T}$ where n_m is the number of fragments of mass m . Quantities of physical interest are easily obtained from the set of partition probabilities. For example, if the sum over partitions is represented as $\Sigma_{\mathbf{n}}$, the mean multiplicity of fragments of mass m (i.e., with m sites) is

$$\langle n_m \rangle = \sum_{\mathbf{n}} n_m(\mathbf{n}) P\{\mathbf{n}\}, \quad (2.1)$$

the mean multiplicity irrespective of mass is $\langle N \rangle = \sum_{m=1}^{M_T} \langle n_m \rangle$ and the mean value of the ejected mass (the total mass minus the mass of the largest fragment observed in a given event) is

$$\langle M \rangle = \sum_{\mathbf{n}} \sum_{m=1}^{\mu_2} m n_m(\mathbf{n}) P\{\mathbf{n}\} = \sum_{\mathbf{n}} [M_T - \mu_1(\mathbf{n})] P\{\mathbf{n}\}, \quad (2.2)$$

where the upper limit, μ_2 , is the mass of the second largest fragment in the event and μ_1 is the mass of the largest fragment. Obviously, $\sum_{m=1}^{\mu_1} m n_m(\mathbf{n}) = M_T$ for all partitions.

We now turn to the results of the simulations and begin by showing, in Fig. 1 (left-hand panel), the probability distributions of the ejected mass. A double peak structure is clearly visible in the transition region (we will discuss the decomposition below). As shown in the upper part of Fig. 2, which refers to simulations with $N_b = 206$ ($N_b/N_T = 0.687$) the left-hand side of this distribution (ejected mass < 60) corresponds to events which include a large residue and for which there are very few fragments of intermediate mass (IMFs, 10–50) whereas the region at the right-hand side (ejected mass > 95) is composed of events in which the residue has disappeared and the probability of observation of IMFs is increased by several orders of magnitude. These characteristics are very similar to those observed recently in the decay of projectile-like fragments (produced in Au-Au system) by the MULTICS-MINIBALL Collaboration [12].

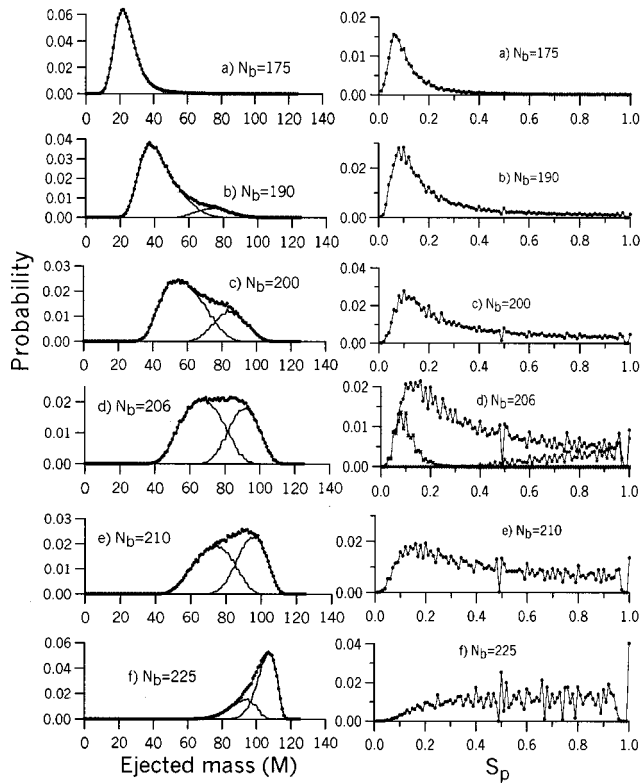


FIG. 1. Left panel: probability distributions of ejected mass, M , for six values of the number of broken bonds in the $5 \times 5 \times 5$ cube. Each distribution is divided into two peaks by classing events with $S_p < 0.4$ and $S_p \geq 0.4$. Right panel: filled circles: probability distributions of the phase separation parameter, S_p . In the spectrum (d) ($N_b = 206$) the crosses and stars represent, respectively, the spectra with gates on the ejected mass of 0–60 and 95–125.

The left-hand panel of Fig. 1 constitutes a direct demonstration of phase coexistence. We further interpret the disappearance of the lower peak and the growth of the second component as striking visual proof of the existence of a phase transition in a small system.

We have also carried out simulations in which the bond breaking probabilities rather than the number of broken bonds were fixed. The results are qualitatively similar to those displayed in Fig. 1 but the spreading introduced in the ejected mass distributions makes the phase transition more difficult to recognize.

In the region where the two peaks overlap we have attempted to separate the phases by defining a phase separation parameter, S_p , as the ratio of the masses of the second largest and largest fragment ($S_p = \mu_2/\mu_1$, right-hand panel of Fig. 1). This choice is based on the fact that, for evaporative-like events, S_p is almost always less than 0.4 [see right panel Figs. 1(a) and (d)]. The division of the ejected mass spectra into groups with S_p greater than or less than 0.4 is indicated in the left-hand panel. The grouping of events following S_p does indeed separate the ejected mass spectrum into lower and upper peaks. Furthermore, as seen in the lower part of Fig. 2 the qualitative characteristics of the partial multiplicity distributions (which are quite different for the two phases) are not affected by including events in the overlap region

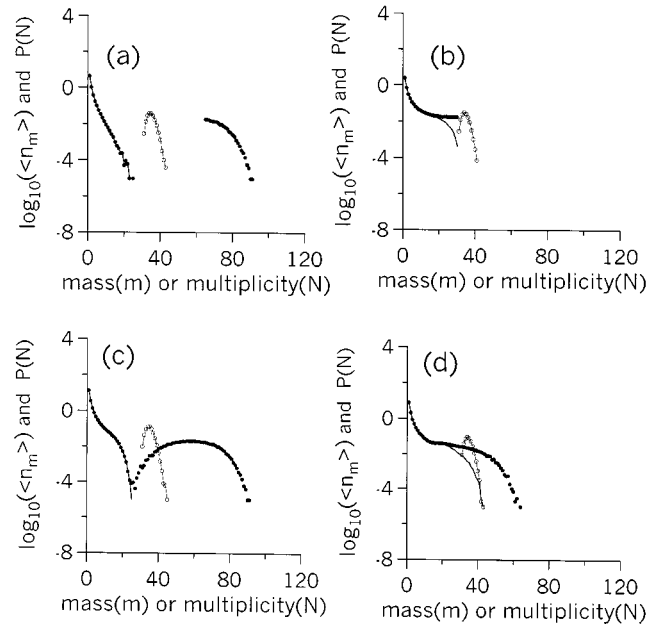


FIG. 2. \log_{10} plots of results of simulations for the $5 \times 5 \times 5$ cube with $N_b = 206$. Filled circles: mean partial multiplicities $\langle n_m \rangle$. Solid line: $\langle n_m \rangle$ values calculated for the same events but with the largest fragment removed from each event. Open circles joined by thin continuous line: probability distributions, $P(N)$ of the total multiplicity, N . (a) with gate on the ejected mass $M \leq 60$; (b) as (a) but with $M \geq 95$; (c) no gate on ejected mass but with $S_p < 0.4$. (d) as (c) but with $S_p \geq 0.4$. [The cutoffs in (a) and (b) are due to the restrictions in the range of M values].

which have assigned following S_p . This being said the “best” value of S_p for separating phases should, of course, be considered as open to some discussion. Changes of the order of 10% do not significantly alter the qualitative characteristics displayed in Figs. 1 and 2.

The two phase decomposition allows us to characterize the individual components of the ejected mass distribution. Thus in Fig. 3(a) we show the first few moments of each peak displayed as a function of the number of broken bonds N_b . The most striking feature is the “speeding up” of the displacement of the centroid of the “residue” phase (phase 1) in the region of the phase transition. The curve is, in fact, almost symmetric and may be considered to play the role of an order parameter. We also observe that the residue phase persists (albeit in rapidly decreasing proportion) even at quite high values of N_b/N_T , a behavior which contrasts with the rapid disappearance of the fragment phase (phase 2) below $N_b/N_T = 0.5$. The lower panel of Fig. 3 [Fig. 3(b)] shows the strong correlation of the total multiplicity with the number of broken bonds. It will be clear from this figure that the multiplicity can be used as a (nonlinear) analog of N_b .

The double peak structure in the ejected mass spectrum is gradually lost as we move to smaller systems. It is not observed in the $3 \times 3 \times 3$ cube. However, we have checked that a broad (flat-topped) structure (rather than a double peak) is observed in a $4 \times 4 \times 4$ cube near the transition.

We now show that it is possible to obtain a strikingly simple characterization of the two phases discussed above.

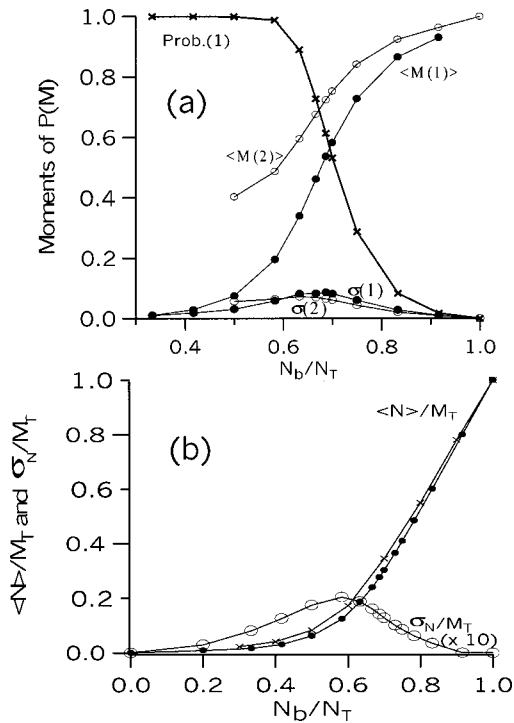


FIG. 3. (a) Probability of phase 1 and mean values and standard deviations of the ejected mass distributions, $P(M)$, for each of the two phases (see left-hand panel of Fig. 1). The moments are plotted as a function of the fraction of broken bonds, N_b/N_T . The mean values and standard deviations have been rescaled (divided by the total number of sites). The second phase disappears below $N_b/N_T = 0.5$. (b) Variation of the mean value (filled circles) and standard deviations (open circles: values shown multiplied by 10) of the total multiplicity, N , with N_b/N_T . The crosses represent data obtained in the $4 \times 4 \times 4$ system.

Phase 1 is, of course, rather simple in structure. There is a large residue left after the dislocation of light particles. A more important observation concerns phase 2. Our simulations indicate that the second phase is obtained simply when the residue itself is broken into two pieces. The evidence for this statement is presented in Fig. 4 in which, for several values of N_b in the region of the transition, we show the ejected mass spectra for phase 1 together with a particular phase 2 mass spectrum constructed by removing both the largest and the second largest fragments. The spectra are almost identical so that the figure strongly suggests that phase 2 corresponds to fission of the residue. Furthermore the corresponding light particle partial multiplicity distributions are very similar except for the heaviest fragments which have very small multiplicities (Fig. 5).

Given the correspondence between characteristics of partition probabilities in percolation and nuclear multifragmentation (see Refs. [1–3]) it seems worthwhile to apply the above results to the nuclear physics case. Indeed it would be most interesting to see how far the analogy can be pursued. Here, we simply resume the difficulties and, where possible, suggest how they may be overcome.

In nuclear physics it is nearly always the case (except at low excitation energies) that only charge partitions are avail-

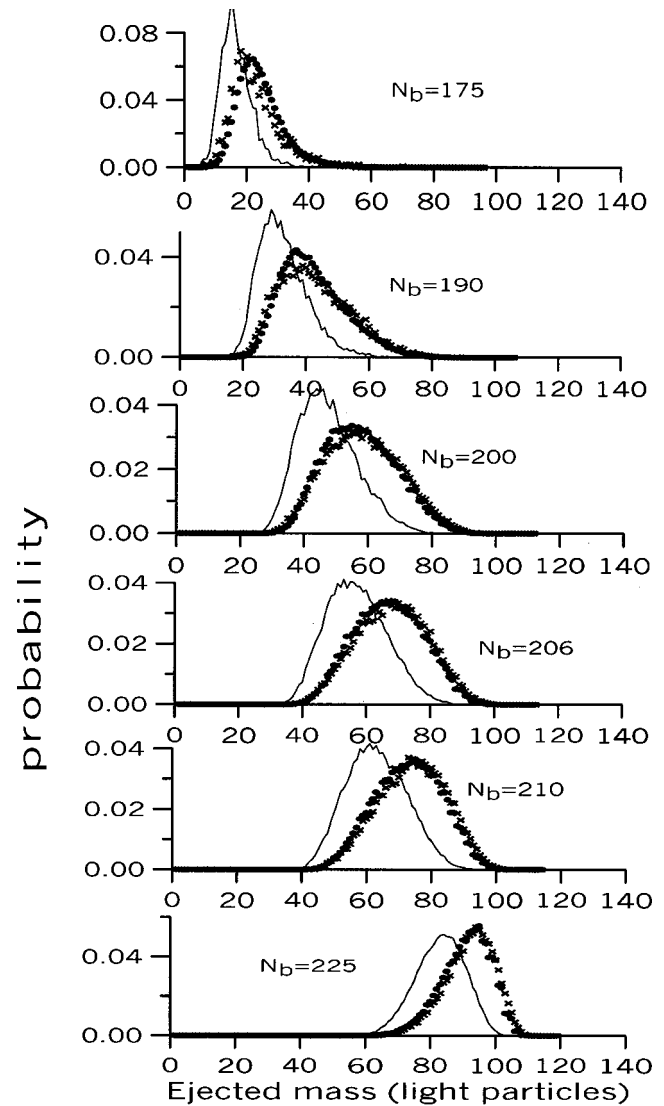


FIG. 4. Mass distributions for several values of N_b . Filled circles: distribution of ejected mass ($M_T - \mu_1$) for phase 1 events. Crosses: the distribution of mass ($M_T - \mu_1 - \mu_2$) for phase 2 events [see text after Eq. (2.2)]. The continuous line which represents the distribution of mass ($M_T - \mu_1 - \mu_2 - \mu_3$) for phase 2 events is not compatible with the ($M_T - \mu_1$) distribution. In all three cases the distributions have been renormalized to unity.

able. While it is certainly true that investigation of specific effects associated with the isospin degree of freedom are well worth undertaking [13] it seems unlikely that the presence of more than one isotope will greatly affect the spectra of ejected charge. This is all the more true when we consider that relatively few isotopes of light and intermediate mass fragments are observed in experiments.

The results described earlier were obtained mainly with simulations involving 10^5 events at each value of N_b (although check runs were performed with 10^6 events). The observation of the transition thus does not require great statistical accuracy. Acceptable spectra may be obtained with only 10^4 events at each value of N_b . This is due simply to the fact that we are dealing with macroscopic variables which may be said to correspond to “gross structure.”

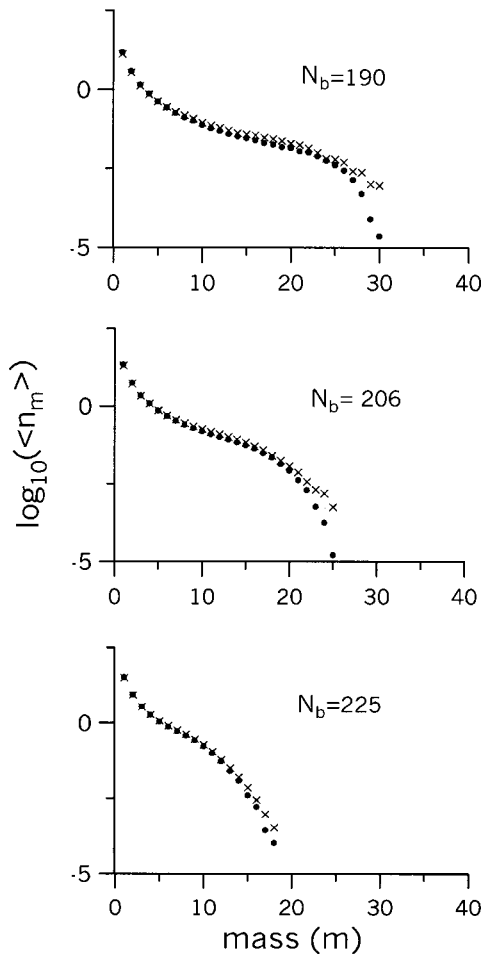


FIG. 5. Distributions of light fragment multiplicities, $\langle n_m \rangle$, in the region of the transition. In this figure the term “light fragments” refers to all fragments except the largest for phase 1 events (filled circles) and all fragments except the largest and second largest for phase 2 events (crosses). In each case the data have been multiplied by renormalization constants to compensate for the variation of the relative probabilities of the two phases.

It appears to be most important to identify a source whose size is essentially fixed. Modern multidetectors are capable of measuring complete events [9,14] and reconstructing such sources so this is probably not a major difficulty especially in view of the preceding remark.

Excited nuclei produced in multifragmentation can be considered as metastable dynamical systems which necessarily decay. If the excitation energies are not too high one speaks of evaporative corrections. In any case what is implied is a long time scale transition of the partition probabilities

$$P'\{\mathbf{n}\} = \sum_{\mathbf{n}'} w(\mathbf{n}, \mathbf{n}') P\{\mathbf{n}'\} + [(1 - W(\mathbf{n})) P\{\mathbf{n}\}], \quad (4.1)$$

where the transition probability, $w(\mathbf{n}, \mathbf{n}')$ is the probability that the partition, \mathbf{n}' , will be transformed into the partition,

\mathbf{n} , by evaporative processes, and $W(\mathbf{n}) = \sum_{\mathbf{n}'} w(\mathbf{n}', \mathbf{n})$. Such a transformation does not take place in percolation. Fragments produced in simulations can be considered as possessing “frozen in” excitation in the sense that the number of unbroken bonds is less than the maximum possible (the binding energy) for the given number of sites [2]. Thus it will be important to investigate, for any particular system, the effect of evaporation corrections. It should be noted that a model set up to calculate the $w(\mathbf{n}, \mathbf{n}')$ can be incorporated into a backtracing procedure [12,15] in order to estimate the pre-evaporation partition probabilities and the corresponding excitation energies from the data.

As shown in Fig. 3(b) the total multiplicity is strongly correlated with the number of broken bonds. This correlation was implicitly invoked by Campi [1] in his analysis of experimental data [16]. It would be useful to check, using current simulation codes [8,17,18], in the nuclear case, to what extent the multiplicity can be used as a measure of intrinsic (as opposed to collective) excitation energy.

In summary, we have presented, in this work, percolation simulations which, via the probability distributions corresponding to the ejected mass, permit the direct observation of the phase transition. We further proposed to separate the two phases using the ratio of the mass of second largest fragment to the mass of the largest fragment (the ratio S_p) in any partition. The results obtained by dividing events into groups with $S_p < 0.4$ and $S_p \geq 0.4$ are consistent with the observation of the transition and with the absence of the second phase at low excitation energy.

We have also shown that, over a large range of the number of broken bonds, N_b , in the region of the transition, the proposed phase separation implies that the second phase corresponds simply to fission of the residue which characterizes the first phase. It would be most interesting to check whether one can identify two phases in nuclear fragmentation which exhibit the same simple structural relation brought to light above.

Finally we have discussed the possible application of the study to nuclear fragmentation. It seems likely that most of the difficulties (in particular that of evaporative corrections) can be overcome using appropriate nuclear fragmentation simulation codes associated with the backtracing technique [15]. A first approach would consist of isolating completely identified events and displaying the ejected mass spectrum as a function of multiplicity.

Both from the percolation and nuclear fragmentation standpoints it would be very interesting to extend this study in order to investigate the properties of the two components in more detail. It would also be highly desirable to make a comparative survey of both lighter and heavier systems. These studies are underway and will be presented in forthcoming works [19].

The author would like to thank P. Désesquelles for a critical reading of the manuscript.

- [1] X. Campi, Phys. Lett. B **208**, 351 (1988).
- [2] A. J. Cole, A. Chabane, M. Charvet, P. Désesquelles, A. Giorni, D. Heuer, A. Lleres, and J. B. Viano, Z. Phys. A **353**, 279 (1995).
- [3] P. Désesquelles, A. J. Cole, A. Giorni, D. Heuer, A. Lleres, J. B. Viano, B. Chambon, B. Cheynis, D. Drain, and C. Pastor, Phys. Rev. C **48**, 1828 (1993).
- [4] A. J. Cole, *Statistical Models for Nuclear Decay* (IOP, Bristol, 2000).
- [5] R. G. Stokstad, in *Treatise on Heavy Ion Science*, Vol. 3, edited by D. A. Bromley (Plenum, New York, 1985).
- [6] O. Lopez, in *Proceedings of the Seventh International Conference on Nucleus-Nucleus Collisions*, edited by W. Nörenberg, D. Guerreau, and W. Mettag [Nucl. Phys. **A685**, 246c (2001)]; J. Richert and P. Wagner, Phys. Rep. **350**, 1 (2001).
- [7] D. H. E. Gross, *Microcanonical Thermodynamics*, Lecture notes in Physics (World-Scientific, Singapore, 2001), Vol. 66.
- [8] J. P. Bondorf, A. S. Botvina, A. S. Iljinov, I. N. Mishustin and K. Sneppen, Phys. Rep. **257**, 133 (1995).
- [9] A. J. Cole, A. Chabane, M. Charvet, P. Désesquelles, A. Giorni, D. Heuer, A. Lleres, J. B. Viano, D. Benckekroun, B. Cheynis, A. Demeyer, E. Gerlic, D. Guinet, M. Stern, and L. Vagneron, Z. Phys. A **356**, 181 (1996).
- [10] J. A. Lopez and J. Randrup, Nucl. Phys. **A503**, 183 (1989); **A512**, 345 (1990).
- [11] D. Stauffer and A. Aharony, *Introduction to Percolation Theory*, 2nd ed. (Taylor and Francis, London, 1985).
- [12] M. D. Agostino *et al.*, MULTICS-MINIBALL Collaboration, Nucl. Phys. **A650**, 329 (1999).
- [13] P. Chomaz, in *Proceedings of the Seventh International Conference on Nucleus-Nucleus Collisions*, edited by W. Nörenberg, D. Guerreau, and W. Mettag [Nucl. Phys. **A685**, 274c (2001)].
- [14] M. E. Brandan *et al.*, Nucl. Instrum. Methods Phys. Res. A **334**, 461 (1993).
- [15] P. Désesquelles, J. P. Bondorf, I. N. Mishustin, and A. S. Botvina, Nucl. Phys. **A604**, 183 (1996).
- [16] C. J. Waddington and P. S. Freier, Phys. Rev. C **31**, 888 (1985).
- [17] Computer code SIMON (unpublished); D. Durand, Nucl. Phys. **A541**, 266 (1992).
- [18] X. Z. Zhang, D. H. E. Gross, S. Y. Xu, and Y. M. Zheng, Nucl. Phys. **A461**, 641 (1987); **A461**, 668 (1987).
- [19] A. J. Cole (in preparation).